A novel acylglycerol kinase that produces lysophosphatidic acid modulates cross talk with EGFR in prostate cancer cells

Meryem Bektas,[1] Shawn G. Payne,[1] Hong Liu,[1] Sravan Goparaju,[1] Sheldon Milstien,[2] and Sarah Spiegel[1]

[1]Department of Biochemistry and the Massey Cancer Center, Virginia Commonwealth University School of Medicine, Richmond, VA 23298
[2]Laboratory of Cellular and Molecular Regulation, National Institute of Mental Health, Bethesda, MD 20892

The bioactive phospholipids, lysophosphatidic acid (LPA) and phosphatidic acid (PA), regulate pivotal processes related to the pathogenesis of cancer. Here, we report characterization of a novel lipid kinase, designated acylglycerol kinase (AGK), that phosphorylates monoacylglycerol and diacylglycerol to form LPA and PA, respectively. Confocal microscopy and subcellular fractionation suggest that AGK is localized to the mitochondria. AGK expression was up-regulated in prostate cancers compared with normal prostate tissues from the same patient. Expression of AGK in PC-3 prostate cancer cells markedly increased formation and secretion of LPA. This increase resulted in concomitant transactivation of the EGF receptor and sustained activation of extracellular signal related kinase (ERK) 1/2, culminating in enhanced cell proliferation. AGK expression also increased migratory responses. Conversely, down-regulating expression of endogenous AGK inhibited EGF- but not LPA-induced ERK1/2 activation and progression through the S phase of the cell cycle. Hence, AGK can amplify EGF signaling pathways and may play an important role in the pathophysiology of prostate cancer.

Introduction

Originally known for its pedestrian role as an intermediate in intracellular lipid metabolism, lysophosphatidic acid (LPA) is now recognized as a potent lipid mediator that evokes growth factor–like responses and regulates an array of cellular processes related to pathogenesis of cancer (Mills and Moolenaar, 2003). Progress in understanding LPA actions has accelerated with the discovery that it is a ligand of several G protein–coupled receptors (GPCRs), termed LPA_1, LPA_2, and LPA_3 (Mills and Moolenaar, 2003). Intriguingly, expression of LPA receptors correlates with more advanced prostate cancer cell lines (Gibbs et al., 2000). In addition to actions through conventional GPCR signaling pathways, LPA receptors can indirectly regulate cell functions by transactivating the EGF tyrosine kinase receptor (Prenzel et al., 1999). This cross-communication between different signaling systems is not only important for the growth-promoting activity of LPA (Prenzel et al., 1999) but it may also be a clue to its pathophysiological role in prostate cancer (Prenzel et al., 1999). The recent discovery that LPA can be generated in the extracellular milieu from lysophosphatidylcholine by the ectoenzyme autotaxin, known to be involved in tumor invasion, neovascularization, and metastasis (Umezu-Goto et al., 2002), further supports the notion that LPA is an important regulator of tumor progression (Mills and Moolenaar, 2003).

A potential pathway for synthesis of LPA is the phosphorylation of monoacylglycerol by a specific lipid kinase (Pieringer and Hokin, 1962), an enzyme that has remained an enigma for more than 40 yr. We have now cloned and characterized a novel acylglycerol kinase (AGK) that phosphorylates both monoacylglycerol to form LPA and diacylglycerol to produce phosphatidic acid (PA), another potent lipid second messenger that mediates mitogenic activation of mTOR (mammalian target of rapamycin) signaling (Fang et al., 2001). LPA produced by AGK in turn activates the EGF receptor, amplifying mitogenic and survival signals and regulating EGF-directed motility. Our results suggest that AGK, which is highly expressed in prostate cancers, might be important for the initiation and progression of prostate cancer, processes in which LPA plays prominent roles (Prenzel et al., 1999; Kue and Daaka, 2000; Kue et al., 2002; Xie et al., 2002; Mills and Moolenaar, 2003).

M. Bektas and S.G. Payne contributed equally to this paper.

Correspondence to Sarah Spiegel: sspiegel@vcu.edu

Abbreviations used in this paper: AGK, acylglycerol kinase; DAG, 1,2-dioleoyl-*sn*-glycerol; DAGK, DAG kinase; ERK, extracellular signal related kinase; GPCR, G protein–coupled receptor; LPA, lysophosphatidic acid; MAGK, monoacylglycerol kinase; MOG, 1-oleoyl-2-*sn*-glycerol; PA, phosphatidic acid; PPARγ, peroxisome proliferator-activated receptor-γ; PTX, pertussis toxin; S1P, sphingosine-1-phosphate; siRNA, small interfering RNA; SphK, sphingosine kinase.

The online version of this article includes supplemental material.

The Journal of Cell Biology, Vol. 169, No. 5, June 6, 2005 801–811
http://www.jcb.org/cgi/doi/10.1083/jcb.200407123

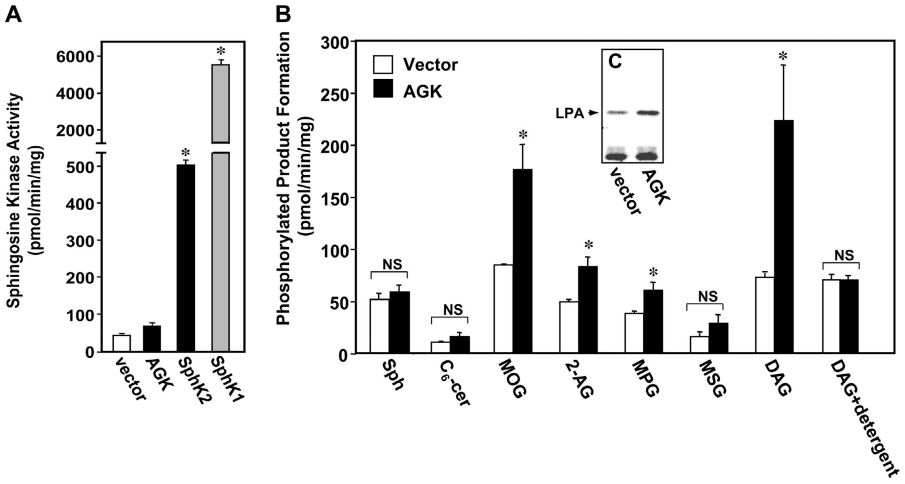

Figure 1. **Lipid kinase activity of recombinant AGK.** (A) NIH 3T3 cells were transiently transfected with vector, hSphK1, hSphK2, or hAGK. After 24 h, cells were lysed and sphingosine-phosphorylating activity in cell lysates was measured with 50 μM D-*erythro*-sphingosine (Sph) substrate added as a BSA complex as described previously (Liu et al., 2000). (B) Lipid-phosphorylating activity was determined in cell lysates from NIH 3T3 cells transiently transfected with vector (open bars) or hAGK (closed bars). The following lipids were tested: Sph, C_6-cer; 1-oleoyl-2-*sn*-glycerol (18:1), MOG; 2-arachidonoyl-glycerol (20:4), 2-AG; 1-palmitoyl-2-*sn*-glycerol (16:0), MPG; 1-stearoyl-2-*sn*-glycerol (18:0), MSG; or diacylglycerol (1,2-dioleoyl-*sn*-glycerol), DAG. Where indicated, octyl-β-glucopyranoside detergent was added to a final concentration of 1.5%. The data are expressed as picomoles of phosphorylated product formed per minute per milligram ± SD. Similar results were obtained in four additional experiments. *, $P < 0.05$ by *t* test. (C) TLC separation of products formed with MOG as substrate visualized with a phosphoimager.

Results

A new lipid kinase catalyzes the phosphorylation of acylglycerols to generate LPA and PA

While searching for additional isoforms of sphingosine kinase (SphK), the enzyme that catalyzes the formation of sphingosine-1-phosphate (S1P), another serum-borne lysophospholipid structurally similar to LPA, we cloned a related gene that encodes a 422–amino acid protein (Fig. S1, available at http://www.jcb.org/cgi/content/full/jcb.200407123/DC1). Although this new kinase was cloned based on its homology to SphKs, it only displayed barely detectable phosphorylating activity with sphingosine as substrate when compared with cells transfected with SphK1 or SphK2 (Fig. 1 A). Moreover, there were no detectable changes in the levels of the sphingolipid metabolites, ceramide, sphingosine, or S1P, in cells overexpressing this lipid kinase. Furthermore, when AGK transfectants were labeled with [^{3}H]sphingosine, there were no significant increases detected in the formation of [^{3}H]S1P compared with vector-transfected cells (unpublished data).

We examined in vitro kinase activity with an array of lipid substrates, including different ceramide species and glycerolipids, such as 1,2-dioleoyl-*sn*-glycerol (DAG), glycerol-3-phosphate, anandamide, phosphatidylinositol, phosphatidylglycerol, cardiolipin, and the monoacylglycerol 1-oleoyl-2-*sn*-glycerol (MOG). Significant phosphorylated products were only detected with monoacylglycerols and diacylglycerols as substrates, but not with any other lipid tested, including ceramide and sphingosine (Fig. 1 B); thus, we have designated this lipid kinase as an AGK. Although AGK contains a DAG kinase (DAGK) catalytic domain (Fig. S1), it did not significantly phosphorylate DAG when activity was measured in the presence of the detergent octyl-β-glucopyranoside (Fig. 1 B), as usually used for DAGK activity measurements (Bunting et al., 1996), suggesting that AGK is distinct from other known DAGKs.

Previously, a partially purified bovine brain monoacylglycerol kinase (MAGK) was reported to prefer substrates containing unsaturated fatty acid esters (Shim et al., 1989; Simpson et al., 1991). Interestingly, AGK has higher activity with substrates containing a C18 fatty acid with one double bond, as monoacylglycerol with an oleoyl (18:1) substitution in the *sn1* position was phosphorylated to a greater extent than 1-palmitoyl-2-*sn*-glycerol (16:0), which was a better substrate than 1-stearoyl-2-*sn*-glycerol (18:0) (Fig. 1 B). Moreover, 1-*sn*-2-arachidonoyl-glycerol, an endogenous cannabinoid receptor ligand (Sugiura et al., 2000), was also a reasonably good substrate (Fig. 1 B). Like the crude bovine brain MAGK activity (Shim et al., 1989), AGK required magnesium for maximal activity, whereas other divalent cations, including Ca^{2+} and Zn^{2+}, inhibited phosphorylation of MOG. Similar to brain MAGK, AGK also had higher activity in the presence of 0.03% deoxycholate, although enzymatic activity was completely abolished by most other detergents, including Triton X-100, Triton X-114, CHAPS, and β-octylglucopyranoside (Fig. 1 B and not depicted).

While this manuscript was in revision, Waggoner et al. (2004) showed that AGK expressed in bacteria phosphorylates DAG as well as MOG and ceramide, but not sphingosine, whereas in lysates of AGK-overexpressing cells, ceramide was not phosphorylated (Fig. 1 B), nor did we detect any phosphorylation of ceramide or sphingosine in vivo.

Subcellular localization of AGK

Confocal immunofluorescence microscopy revealed that AGK was distributed in a punctate, reticular pattern in NIH 3T3 cells (Fig. 2 A), which is reminiscent of a mitochondrial localization. There was no significant colocalization with the ER marker calnexin (Fig. 2 A). On the other hand, AGK expression clearly colocalized with mitochondria stained with MitoTracker red (Fig. 2 A). Similar mitochondrial localization of AGK was also observed in HEK 293 and PC-3 cells (Fig. S2 A, available at http://www.jcb.org/cgi/content/full/jcb.200407123/DC1), indicating that the subcellular distribution was not cell type specific. In agreement, although AGK does not contain a canonical mitochondrial localization signal, the MitoProt II website predicts an 80% probability of mitochondrial localization,

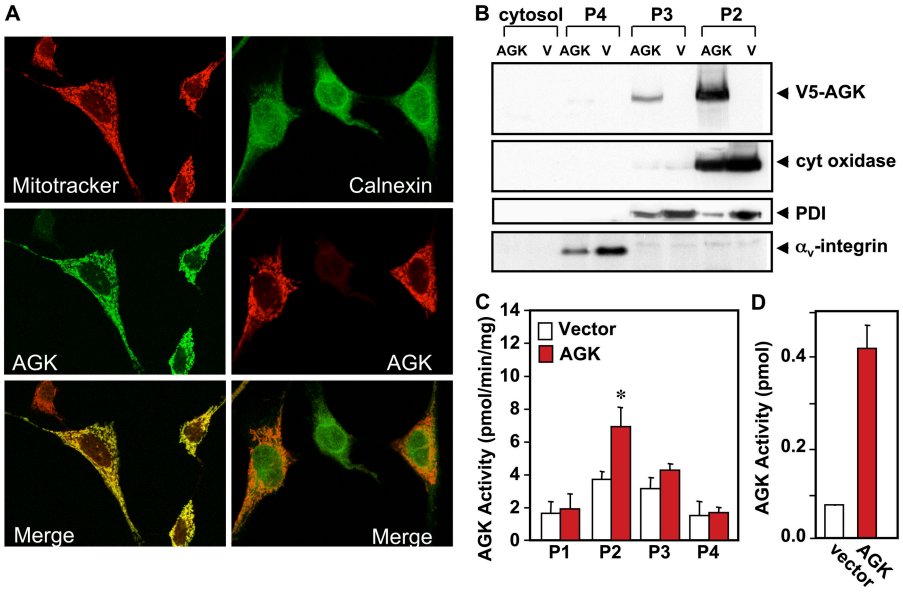

Figure 2. **Subcellular localization of AGK.** (A) NIH 3T3 fibroblasts were transiently transfected with V5-tagged AGK and mitochondria stained with MitoTracker red. The ER was visualized with anti-calnexin antibody followed by FITC-conjugated anti-rabbit as the secondary antibody. AGK was stained with monoclonal anti-V5 antibody followed by secondary FITC-conjugated or Texas red–conjugated anti–mouse antibody. Cells were visualized by dual wavelength confocal microscopy. Superimposed merged pictures are shown in the bottom panels, with yellow indicating colocalization. (B and C) Activity and expression of AGK in subcellular fractions. Lysates from HEK 293 cells transfected with vector or V5-AGK and P2 (mitochondria), P3 (ER and Golgi), P4 (plasma membrane), and cytosol fractions isolated. The P1 fraction containing nuclei and unbroken cells was not examined. 25 μg of proteins were resolved by SDS-PAGE and immunoblotted with anti-V5 antibody or with antibodies to the specific organelle markers anti–cytochrome *c* oxidase, anti-phosphodisulfide isomerase (PDI), and anti–α_v-integrin. AGK activity was also determined in each subcellular fraction with MOG as substrate. Results are means ± SD of triplicate determinations. Similar results were obtained in two additional experiments. *, $P < 0.05$ by *t* test. (D) 400-μg aliquots of lysates from HEK 293 cells transiently transfected with vector (open bars) or V5-AGK (closed bars) were immunoprecipitated with anti-V5 antibody as described in Materials and methods, and AGK activity was determined in the immunoprecipitates. Data are expressed as picomoles of LPA formed in 30 min and are means ± SD of duplicate determinations.

and the program TMpred predicted one transmembrane region from amino acid 11 to 30.

To further substantiate the localization of AGK, protein expression and enzymatic activity were examined in subcellular fractions prepared by differential centrifugation. V5-Epitope–tagged AGK with the predicted MW of 46.4 kD was highly enriched in the P2 mitochondria fraction (Fig. 2 B). Much less AGK was present in the P3 fraction containing intracellular membranes of the ER and Golgi or in the P4 plasma membrane fraction. In concordance with the protein expression pattern, the highest AGK-specific activity was in P2 (Fig. 2 C).

AGK regulates LPA and PA in vivo

To definitively demonstrate that AGK has intrinsic kinase activity rather than affecting the activity of some endogenous lipid kinase, phosphorylation of acylglycerol substrates after specific pull-down of epitope-tagged AGK expressed in HEK 293 cells with V5 antibody was determined. Although the V5 antibody inhibits AGK, phosphorylation of MOG was sixfold greater in immunoprecipitates from V5-AGK transfectants than vector transfectants (Fig. 2 D) and there was no significant phosphorylating activity with other lipid substrates (not depicted).

To identify the phosphorylated lipids produced by AGK in vivo, vector and AGK PC-3 transfectants were incubated with ^{32}P-labeled orthophosphate and labeled phospholipids in isolated mitochondria examined (Fig. 3 A). Expression of AGK resulted in 80% increase of ^{32}P-labeled PA without significantly affecting labeling of the other mitochondrial phospholipids. Because it is known that LPA synthesized in mitochondria can readily exit this organelle (Chakraborty et al., 1999) or be rapidly metabolized to PA, changes in total cellular phospholipids were also examined (Fig. 3, B–D). There were no obvious differences in labeling of the major known cellular phospholipids in AGK-expressing cells compared with the vector cells. However, two-dimensional HPTLC analysis revealed that a labeled phospholipid that comigrated with authentic LPA (Fig. 3, B and C), although barely detectable in vector cells, was increased threefold in AGK-expressing cells. Moreover, this phospholipid was eliminated by treatment with phospholipase B, which hydrolyzes the ester bonds of lysophospholipids, confirming its identity as LPA. Labeled PA was also increased in these transfectants (Fig. 3 D), albeit much less than LPA. Of note, in these cells, AGK mRNA levels relative to 18S RNA were increased by almost twofold over endogenous expression from 1.2 ± 0.1 to 2.3 ± 0.2, as determined by quantitative PCR.

It has previously been shown that cancer cells secrete LPA (Mills and Moolenaar, 2003). Small amounts of labeled lysophospholipids, including LPA, were secreted by vector transfected PC-3 cells. However, secretion of ^{32}P-labeled LPA was significantly increased threefold by overexpression of AGK (Fig. 3, F and G), indicating that AGK increases both intracellular and extracellular levels of LPA. It should be noted that AGK was not detectable in the medium by immunoblotting nor did its expression cause apoptosis of cells, suggesting that appearance of LPA in the media is not a result of cell death.

All members of the DAGK and SphK superfamily have a conserved GDG sequence in the glycine-rich loop of the putative ATP binding region and a single point mutation of the second conserved glycine residue to aspartate has been used to prepare catalytically inactive DAGK (Topham and Prescott, 1999) and SphK (Pitson et al., 2002). Similarly, site-directed mutagenesis of the equivalent residue in AGK (G126E) resulted in a complete loss of phosphorylating activity (Fig. S2 B), and its expression had no discernible effects on ^{32}P-labeled LPA, PA, or other phospholipids (Fig. S2 C). However, like wild-type AGK, this catalytically inactive mutant was localized to the mitochondria (Fig. S2 A)

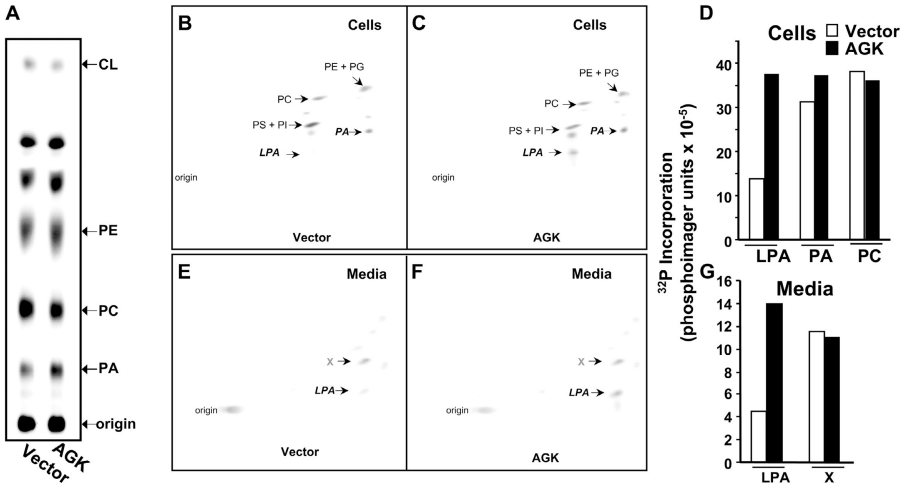

Figure 3. **Effect of AGK on phospholipids.** (A) PC-3 cells stably transfected with vector or AGK were labeled with ^{32}P-orthophosphate for 2 h. Phospholipids were then extracted from mitochondria isolated by differential centrifugation. After separation of equal amounts of ^{32}P-labeled phospholipids by one-dimensional TLC, radioactive spots were visualized with a phosphoimager and the indicated lipids were identified based on comigration with authentic standards. The ratio of ^{32}P-PA to ^{32}P-PC in vector and AGK transfectants was 0.38 ± 0.02 and 0.68 ± 0.03, respectively. (B–G). LPA production and secretion induced by expression of AGK. PC-3 cells stably transfected with vector or AGK were prelabeled with ^{32}P-orthophosphate for 2 h, washed, and incubated for 2 h in chemically defined medium. Lipids were extracted from cells (B–D) and media (E–G). Equal amounts of ^{32}P-phospholipids were separated by two-dimensional HPTLC, first in chloroform/methanol/formic acid/water (60:30:7:3, vol/vol), followed by chloroform/methanol/ammonium hydroxide/water (50:40:8:2, vol/vol). Radioactive spots were visualized with a phosphoimager, and the indicated lipids were identified based on comigration with authentic standards. (D and G) ^{32}P incorporation into the indicated phospholipids (LPA, PA, PC, and unidentified phospholipid [X]) was quantified by phosphoimager. Similar results were obtained in two additional experiments.

AGK is highly expressed in prostate cancer

As LPA has been most prominently associated with growth-promoting effects and probably contributes to cancer (Mills and Moolenaar, 2003), it was of interest to examine the expression of AGK in normal tissues and cancers. By Northern analysis, a 2.6-kb AGK mRNA was widely expressed (Fig. 4 A), most abundantly in heart, kidney, muscle, and brain. Importantly, using a matched human tumor/normal tissue expression array, we found that AGK expression was significantly up-regulated in prostate cancers compared with the normal prostate tissues from the same patient (Fig. 4 B). However, not all tumor tissues show an increase in AGK expression. In uterine, cervical, and stomach cancers, there also appeared to be higher expression of AGK compared with the normal tissues, whereas AGK expression seems to be reduced in colon cancer. AGK was also expressed in many types of human cancer cell lines (Fig. 4 B), including prostate cancer cells, such as androgen-responsive LNCaP cells, which are more similar to early stage carcinoma, and androgen-insensitive TSU-Pr1 and PC-3 cells, a model for more advanced prostate carcinoma.

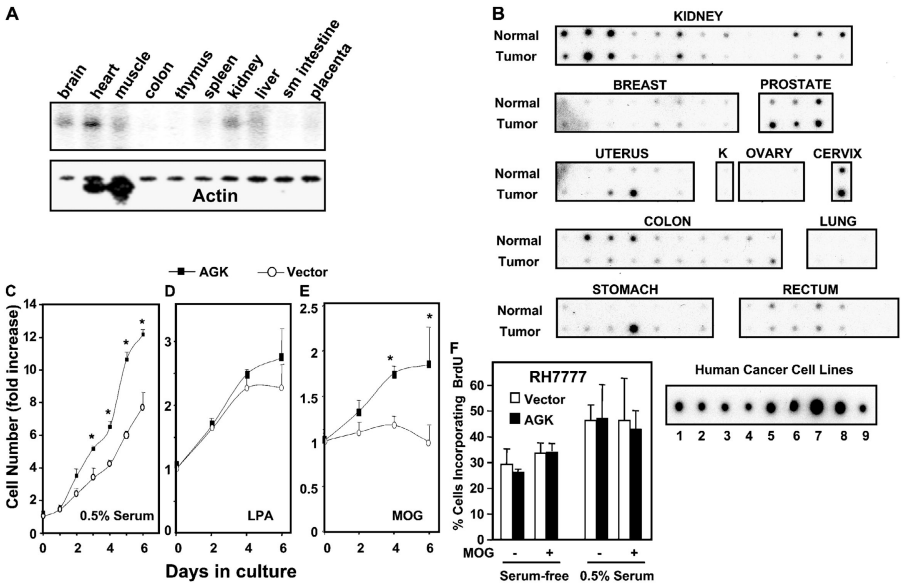

Figure 4. **Expression of hAGK.** (A) Northern blot analysis of hAGK expression in human tissues. Random labeled probe was hybridized to poly(A)$^+$ RNA blots from the indicated human tissues. β-Actin expression was used to confirm equal loading. (B) Matched tumor/normal array analysis of hAGK expression. An array containing cDNA samples from multiple tissues and tumor types as well as nine cancer cell lines was probed with ^{32}P-labeled AGK probe. Each pair of tumor and normal samples came from the same patient. Human cancer cell lines: (1) HeLa; (2) Burkitt's lymphoma, Daudi; (3) chronic myelogenous leukemia; (4) promyelocytic leukemia HL-60; (5) melanoma; (6) lung carcinoma; (7) lymphoblastic leukemia, MOLT-4; (8) colorectal adenocarcinoma, SW480; (9) Burkitt's lymphoma, Raji. There was no specific hybridization to the control nucleic acids, which included ubiquitin cDNA, yeast total RNA, yeast tRNA, *Escherichia coli* DNA, poly(A), human C_ot-1 DNA, and human genomic DNA. (C–E) AGK stimulates proliferation. PC-3 cells stably transfected with vector (open symbols) or AGK (closed symbols) were cultured in serum-free medium supplemented with 0.5% serum (C), 10 μM LPA (D), or 10 μM MOG (E), and cell numbers determined at the indicated days. Data are expressed as fold increase relative to day 0 and are means ± SD. Similar results were obtained in two additional experiments. Asterisks denote significant differences ($P < 0.05$, *t* test). (F) AGK does not enhance proliferation of RH*7777* cells. RH*7777* cells were cotransfected with vector (open bars) or AGK (closed bars) together with GFP at a ratio of 4:1. After 24 h, cells were cultured in serum-free medium or in the presence of 0.5% serum. BrdU was added 16 h later for an additional 3 h. Double immunofluorescence was used to visualize transfected cells and BrdU incorporation into nascent DNA. The proportion of cells incorporating BrdU among total GFP transfected cells was determined. Data are means ± SD of triplicate cultures from a representative experiment. At least three different fields with a minimum of 100 cells/field were scored.

AGK expression enhances cell growth through LPA receptors

Growth promotion is one of the most prominent effects mediated by LPA (Mills and Moolenaar, 2003). Consistent with its ability to increase LPA synthesis, transient or stable expression of AGK enhanced proliferation of diverse cell types, including PC-3 cells (Fig. 4, C–E) and NIH 3T3 fibroblasts (Fig. S3 A, available at http://www.jcb.org/cgi/content/full/jcb.200407123/DC1). The growth-promoting effect of AGK was observed even in the presence of suboptimal serum concentrations (Fig. 4 C and Fig. S3 A). Although AGK stimulates growth, it had no cytoprotective effects on apoptosis induced by serum deprivation or the anti-cancer drug doxorubicin (Fig. S3 D). As expected, exogenous LPA increased proliferation of both AGK and vector transfectants to the same extent (Fig. 4 D). Addition of MOG to cells cultured in serum-free medium had a minimal effect on vector transfectants and significantly stimulated proliferation of AGK-expressing PC-3 cells (Fig. 4 E). This result is probably due to rapid metabolism and degradation of MOG, and thus only in AGK-expressing cells is sufficient LPA produced and secreted (Fig. 3, F and G) to stimulate proliferation.

FACS analysis revealed that 83 ± 0.4% of the vector transfectants were in Go/G1 phase and 7.0 ± 0.04 and 10 ± 0.4% were in S and G2/M phases, respectively. Overexpression of AGK reduced the fraction of cells in Go/G1 to 73 ± 0.1% and increased the proportion in the S phase by greater than twofold (15 ± 0.1%), without significantly affecting the proportion in the G2/M phase (12 ± 0.1%).

Although it is well established that the mitogenic effects of LPA in many cell types are mediated by binding to its specific GPCRs (Mills and Moolenaar, 2003), intracellular actions have also been suggested (Hooks et al., 2001), possibly as an agonist of the nuclear transcription factor peroxisome proliferator-activated receptor-γ (PPARγ; Zhang et al., 2004). To examine the potential involvement of intracellular actions of LPA generated by expression of AGK, its mitogenic effects were examined in rat hepatoma RH7777 cells that do not express $LPA_{1\text{-}4}$ and do not respond to LPA (Fukushima et al., 1998). However, in contrast to PC-3 (Fig. 4, C–E) and NIH 3T3 (Fig. S3 A) cells, RH7777 cells did not show an increase in DNA synthesis in response to expression of AGK as measured by incorporation of BrdU into nascent DNA (Fig. 4 F). Although RH7777 cells express AGK, it is possible that they do not produce sufficient amounts of LPA if MOG is limiting. However, even addition of MOG did not enhance BrdU incorporation in RH7777 cells expressing AGK (Fig. 4 F).

Similar to a previous paper (Lea et al., 2004), GW9662, a selective antagonist of PPARγ, inhibited proliferation of PC-3 cells (Fig. 5 A). However, importantly, it did not abrogate the mitogenic effect of AGK (Fig. 5 A). Consistent with previous studies (Kue et al., 2002), we found that LPA_1, LPA_2, and LPA_3 are expressed in PC-3 cells (unpublished data). It is known that LPA_1 couples to pertussis toxin (PTX)–sensitive Gi, whereas LPA_2 and LPA_3 couple also to Gq. In PC-3 cells, LPA-regulated mitogenic signaling is mediated by Gβγ subunits derived from PTX-sensitive Gi proteins (Bookout et al., 2003). In agreement, PTX pretreatment not only inhibited growth of vector transfectants but it also markedly decreased the growth-promoting effects of AGK (Fig. 5 A). However, AGK expression enhanced cell proliferation even in the presence of PTX.

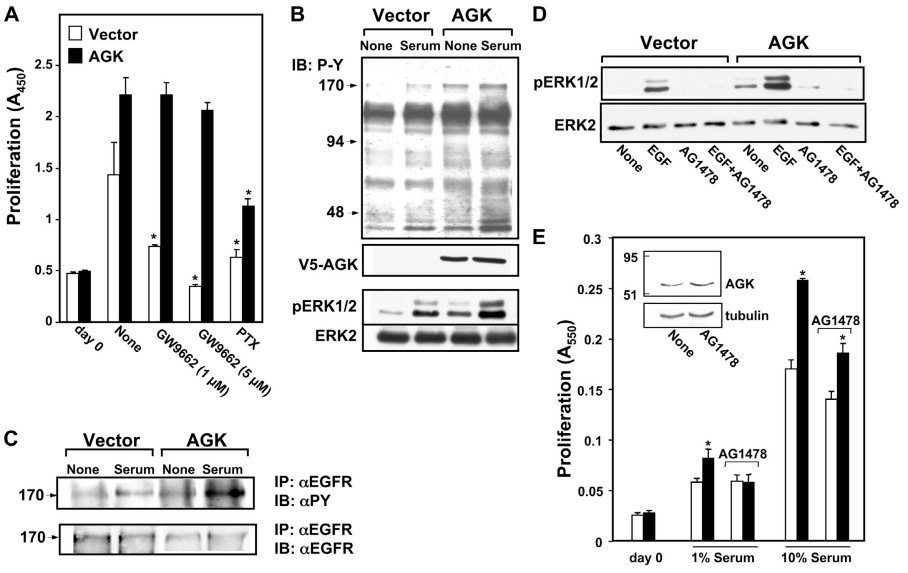

Figure 5. **Regulation of cell growth and EGFR signaling by AGK.** (A) Effect of PTX and the PPARγ antagonist GW9662 on AGK-induced proliferation. PC-3 cells stably transfected with vector (open bars) or AGK (closed bars) were cultured in medium supplemented with 1% serum without or with GW9662 (1 μM or 5 μM) or with PTX (100 ng/ml), and cell proliferation was determined after 6 d with WST-1. Asterisks denote significant differences compared with untreated controls ($P < 0.05$, *t* test). (B) Enforced expression of AGK enhances EGFR tyrosine phosphorylation and stimulates ERK1/2. Serum-starved PC-3 cells stably transfected with vector or AGK were stimulated without or with 10% serum for 10 min, lysed and immunoblotted with anti-phosphotyrosine, anti-V5 antibody, or phospho-specific anti-ERK1/2 antibodies. Blots were stripped and reprobed with ERK2 antibody to demonstrate equal loading. (C) AGK expression induces EGFR transactivation. Lysates from cells treated as in B were immunoprecipitated with anti-EGFR antibody and the immunoprecipitates were analyzed by Western blotting using anti-phosphotyrosine or anti-EGFR antibody. (D and E) Blockage of EGFR signaling suppresses ERK activation and cell growth advantage mediated by AGK. (D) Serum-starved PC-3 cells stably transfected with vector or AGK were preincubated for 60 min in the absence or presence of 200 nM AG1478, and then treated with EGF for 10 min. Cell lysate proteins were analyzed by immunoblotting with phospho-specific ERK1/2 antibody. Blots were stripped and reprobed with ERK2 antibody to demonstrate equal loading. (E) PC-3 cells stably transfected with vector or AGK were cultured in medium supplemented with 1 or 10% serum with or without 200 nM AG1478, and cell proliferation was determined after 6 d with crystal violet. Similar results were obtained in two additional experiments. Asterisks denote significant differences ($P < 0.05$, *t* test). (inset) PC-3 cells stably transfected with V5-AGK were incubated for 6 d without (None) or with AG1478, and AGK expression was determined by immunoblotting with anti-V5 antibody. The blot was stripped and reprobed with anti-tubulin as a loading control.

AGK promotes transactivation of EGFR

Many studies have led to the notion that LPA is important in the pathophysiology of prostate carcinoma functioning in an emerging paradigm of cross talk between LPA receptors and the tyrosine kinase EGFR (Prenzel et al., 1999; Mills and Moolenaar, 2003). Therefore, it was of importance to determine whether overexpression of AGK and increased LPA levels resulted in such receptor transactivation leading to enhanced growth.

In serum-starved cells, AGK expression increased tyrosine phosphorylation of several proteins, notably a 170-kD band, which was similarly increased by serum in vector transfectants (Fig. 5 B). Kinetic analysis revealed that the 170-kD tyrosine phosphorylation induced by serum was a rapid event in AGK-expressing cells, clearly evident within 5 min and remaining elevated for at least 60 min (Fig. S4 A, available at http://www.jcb.org/cgi/content/full/jcb.200407123/DC1). The enhanced tyrosine phosphorylation of the 170-kD protein represented activation of the EGFR, as immunoblotting of anti-EGFR immunoprecipitates with anti-phosphotyrosine revealed increased EGFR tyrosine phosphorylation in cells overexpressing AGK, even in the absence of serum (Fig. 5 C).

AGK-induced extracellular signal related kinase (ERK) 1/2 activation requires EGFR

Previously, it has been suggested that EGFR activation is required for signal relay from LPA receptors to ERK1/2 activation in prostate cancer cells (Prenzel et al., 1999; Kue et al., 2002; Raj et al., 2002). AGK expression markedly increased activation of ERK1/2, as determined with a phospho-specific antibody, which was further enhanced by serum (Fig. 5 B) and EGF (Fig. 5 D and Fig. S3 C). To further confirm that activation of the EGFR was necessary for AGK-stimulated ERK activation, we used the specific EGFR tyrosine kinase inhibitor, tyrphostin AG1478. As expected, AG1478 abolished EGFR-induced tyrosine phosphorylation (Fig. S4 B). AG1478 blocked AGK-mediated ERK1/2 phosphorylation (Fig. 5 D) and decreased its mitogenic effect (Fig. 5 E) and also inhibited MOG-stimulated proliferation by 35 ± 4%. Nonetheless, prolonged treatment with AG1478 did not affect AGK protein levels (Fig. 5 E, inset).

Involvement of AGK in motility

Transactivation of the EGFR has also been implicated in motility of cancer cells (Gschwind et al., 2001). In agreement, AGK overexpression enhanced migration of PC-3 cells toward EGF, which was blocked by the EGFR inhibitor AG1478 (Fig. 6 A). AGK also enhanced migration of NIH 3T3 fibroblasts toward serum (Fig. S3 B).

In the Boyden chamber cell migration assay, differences in cell shape and size may affect passage through the pores in the membrane but do not affect the in vitro wound closure assay. AGK expression also enhanced closure of the wounded area, especially in the presence of EGF and the AGK substrate MOG (Fig. 6, B and C). In contrast, wound closure induced by LPA was not affected by AGK expression. AGK-induced wound closure was also blocked by AG1478, supporting a role for EGFR transactivation in AGK-induced migratory responses.

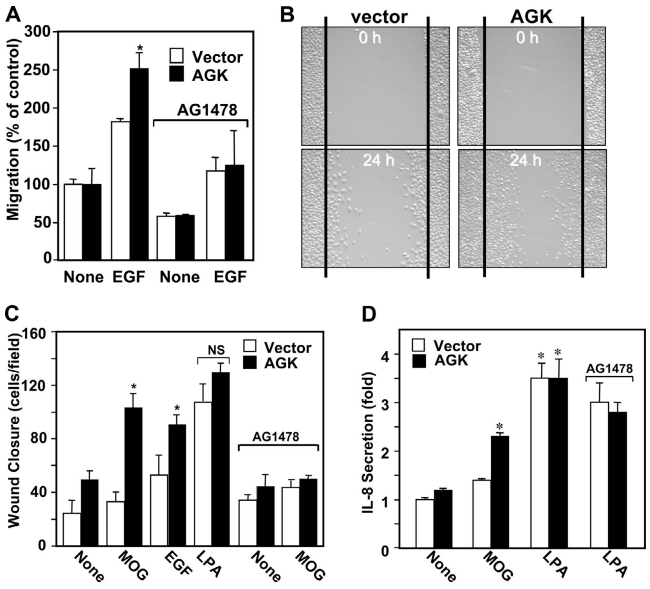

Figure 6. **EGFR is required for AGK-stimulated cell migration toward EGF and wound closure.** (A) PC-3 cells transfected with vector (open bars) or AGK (closed bars) were pretreated without or with 200 nM AG1478 for 20 min and allowed to migrate for 3 h toward EGF (10 ng/ml). The data are means ± SD of two determinations. Similar results were obtained in two independent experiments. (B and C) Monolayers of vector (open bars) or AGK (closed bars) PC-3 transfectants were wounded and treated with vehicle, MOG (10 μM), LPA (10 μM), or EGF (10 ng/ml). Where indicated, cells were also treated with 200 nM AG1478. (B) Representative images of a wound healing assay with vector and AGK-transfected PC-3 cells before and 24 h after treatment with MOG. (C) Migration of cells into the wound was determined after 24 h by processing digital photographs with ImagePro Plus. (D) AGK induces IL-8 secretion. PC-3 cells transfected with vector (open bars) or AGK (closed bars) were serum starved for 24 h and treated in serum-free DME with or without MOG (10 μM) or LPA (1 μM) for 16 h, and IL-8 secretion was measured by ELISA. Where indicated, cells were also treated with 200 nM AG1478. *, $P < 0.05$ by *t* test.

AGK up-regulates IL-8

Expression of the multifunctional cytokine IL-8 correlates with angiogenesis, tumorigenicity, and metastasis of human prostate cancer cells implanted in nude mice (Kim et al., 2001). Similarly, LPA markedly enhanced IL-8 secretion from PC-3 cells. Expression of AGK slightly increased IL-8 release, which was further significantly increased by addition of MOG, the precursor of LPA (Fig. 6 D). The EGFR inhibitor AG1478 only slightly decreased LPA-induced IL-8 secretion, suggesting that this response is independent of EGFR transactivation.

Involvement of endogenous AGK in ERK1/2 activation and cell cycle progression

Serum and EGF induced significant increases in AGK expression as determined by quantitative real-time PCR (Fig. 7 A). It has previously been shown that LPA itself is sufficient to increase its own production in PC-3 cells, indicating the pres-

ence of an autocrine network (Qi et al., 1998). Consistent with an autocrine function for LPA, we found that LPA also increased expression of AGK by threefold in naïve PC-3 cells (Fig. 7 A). To examine the physiological function of AGK, its expression was down-regulated with small interfering RNA (siRNA). siAGK, but not control siRNA, markedly reduced AGK mRNA in PC-3 cells, as determined by QPCR, without influencing expression of SphK1 (Fig. 7 B). Consistent with its role in synthesis of LPA and PA, the most striking effect of down-regulating AGK was reduction of mitochondrial PA and LPA by ~30% (Fig. 7 C). Remarkably, siAGK completely blocked stimulation of ERK1/2 induced by EGF (Fig. 7 D). To rule out off-target effects, we used two additional unrelated siRNAs targeted to different sequences of AGK. $siAGK_2$ and $siAGK_3$ markedly and specifically reduced expression of AGK determined by QPCR (0.2 and 0.16 relative to siControl) without reducing expression of SphK1 (1.1 and 1.0 relative to siControl) or SphK2 (1.1 and 1.0 relative to siControl). Importantly, both of these siRNAs also markedly reduced EGF-induced ERK1/2 activation but did not decrease LPA-induced ERK activation (Fig. 7 E), suggesting that LPA can bypass the effects of down-regulation of AGK. In addition, down-regulation of AGK reduced EGF-stimulated tyrosine phosphorylation of the EGFR (Fig. S3 C).

Down-regulation of AGK reduced EGF-induced wound closure but had no effect on wound closure induced by LPA (Fig. 7 F). siAGK also reduced migration toward EGF but not toward serum (Fig. 7 G). siAGK but not siControl inhibited basal secretion of IL-8 in untreated PC-3 cells and also blocked the small effect of MOG (1.28- and 1-fold stimulation in siControl and siAGK, respectively; Fig. 7 H). However, its effects on EGF or LPA-induced IL-8 secretion were smaller (fold stimulation with EGF is 2.16 and 2.06 and with LPA is 5 and 7.5 in siControl and siAGK, respectively). Similarly, $siAGK_2$ also reduced basal IL-8 secretion without affecting LPA-induced secretion (Fig. 7 H).

Next, we examined the role of endogenous AGK in cell growth regulation. The levels of LPA in serum range from 1 to 6 μM (Baker et al., 2001), and in 10% serum, the level is well below the concentration needed for its mitogenic effects. In agreement with others (Qi et al., 1998), we have found that serum is a more potent mitogen for PC-3 cells than 10 μM LPA (unpublished data). Remarkably, siAGK markedly decreased DNA synthesis as measured by incorporation of BrdU into nascent DNA, whereas nonspecific siRNA had no effect (Fig. 8, A and B). In agreement, cell cycle analysis revealed that after one day in serum-free medium, >75% of PC-3 cells transfected with nonspecific siRNA were in G_o/G_1 phase and only a small fraction were in S and G_2/M phases, which was similar to untreated cells (Fig. 8 C and not depicted). Transfection with siAGK increased the fraction of cells in G_o/G_1 and decreased the proportion in the S phase and the G_2/M phase. In the presence of 10% serum, which markedly increased the proportion of cells in the S phase and G_2/M phase, siAGK, but not control siRNA, further reduced cells in S phase, albeit to a lesser extent than in the absence of serum (Fig. 8 C).

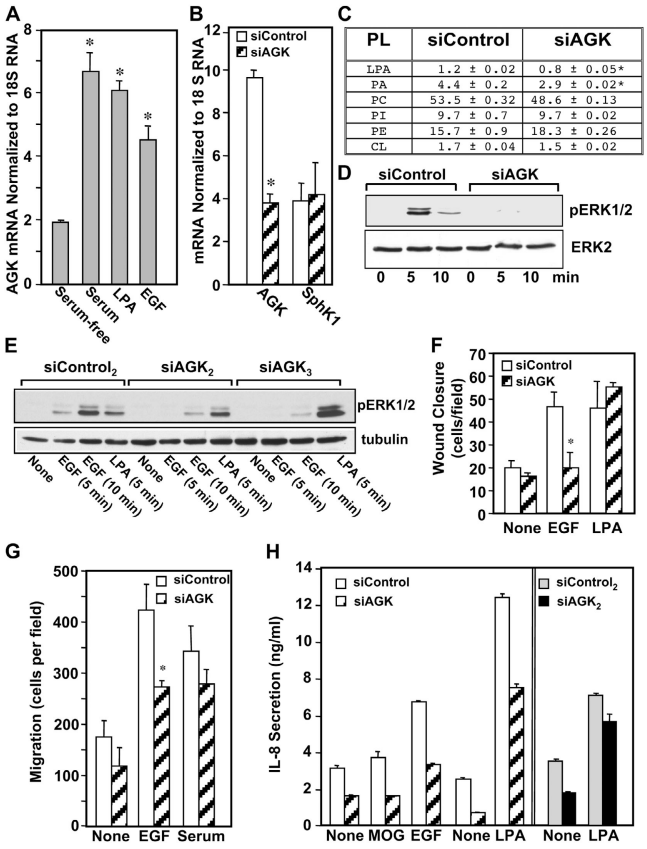

PL	siControl	siAGK
LPA	1.2 ± 0.02	0.8 ± 0.05*
PA	4.4 ± 0.2	2.9 ± 0.02*
PC	53.5 ± 0.32	48.6 ± 0.13
PI	9.7 ± 0.7	9.7 ± 0.02
PE	15.7 ± 0.9	18.3 ± 0.26
CL	1.7 ± 0.04	1.5 ± 0.02

Figure 7. **Effectiveness and specificity of siAGK.** (A) Expression of endogenous AGK. Naïve PC-3 cells were serum starved for 24 h and treated in DME with or without 10% serum, LPA (10 μM), or EGF (100 ng/ml) for 16 h, and AGK mRNA was determined by quantitative real-time PCR. Data were normalized to expression of 18S RNA and are means ± SD of triplicate determinations. *, $P < 0.05$ by *t* test. (B) PC-3 cells were transfected with control siRNA (open bars) or siRNA specific for AGK (hatched bars) and mRNA levels of AGK and SphK1, and 18S RNA was determined by QPCR. (C) Duplicate cultures were labeled with ^{32}Pi for 12 h. Phospholipids were extracted from mitochondria isolated by differential centrifugation. Equal amounts of ^{32}P-phospholipids were separated by TLC, and the indicated phospholipids were quantified with a phosphoimager. The data are expressed as a percentage of total ^{32}P-labeled phospholipids and are means ± SD of duplicate determinations. *, $P < 0.05$ by *t* test. (D) Down-regulation of AGK with siRNA blocks EGF-induced ERK1/2. PC-3 cells were transfected with control siRNA or siRNA specific for AGK and treated without (None) or with 10 ng/ml EGF for the indicated times. Equal amounts of lysate proteins were separated by SDS-PAGE, and ERK1/2 activation was determined by immunoblotting with anti-pERK1/2. Blots were stripped and reprobed with anti-ERK2 as a loading control. (E) PC-3 cells were transfected with $siControl_2$, $siAGK_2$, or $siAGK_3$ (Dharmacon), as described in Materials and methods, and treated with EGF (10 ng/ml) or LPA (10 μM) for the indicated times. Equal amounts of lysate proteins were separated by SDS-PAGE and ERK1/2 activation determined by immunoblotting with anti-pERK1/2. Blots were stripped and reprobed with anti-tubulin as a loading control. Down-regulation of AGK decreases EGF-induced wound closure and migration. (F) Monolayers of PC-3 cells transfected with control siRNA (open bars) or siRNA specific for AGK (hatched bars) were wounded and treated with vehicle (None), EGF (10 ng/ml), or LPA (10 μM), and migration of cells into the wound was determined after 24 h. (G) Cells from duplicate cultures were allowed to migrate for 3 h in Boyden chambers toward vehicle (None), EGF (10 ng/ml), or serum (10%). The data are means ± SD of two determinations. (H) Down-regulation of AGK with siRNA decreases IL-8 secretion. PC-3 cells were transfected with the indicated control siRNAs (open bars and gray bars) or siRNAs specific for AGK (hatched bars and black bars), incubated in serum-free DME without (None) or with MOG (10 μM), LPA (1 μM), or EGF (10 ng/ml) for 16 h, and IL-8 secretion was measured. *, $P < 0.05$ by *t* test.

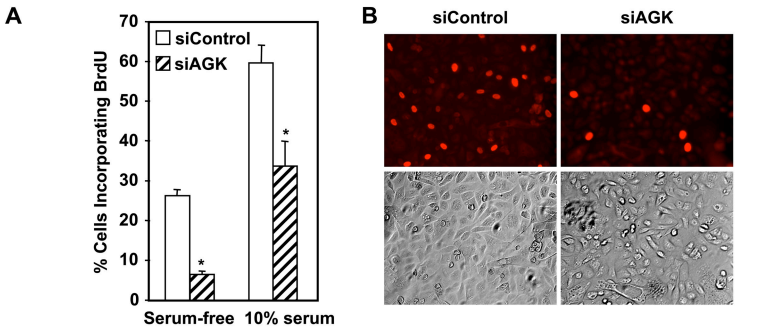

C

	Cells	G_o/G_1	S	G_2/M
Serum-free	siControl	75.1 ± 2.3	12.5 ± 2.0	12.4 ± 1.3
	siAGK	**83.8 ± 1.9**	**6.8 ± 1.4 ***	**9.4 ± 0.6***
10% Serum	siControl	54.8 ± 0.6	22.9 ± 0.5	22.3 ± 0.1
	siAGK	**64.3 ± 0.8**	**16.3 ± 0.6 ***	**19.4 ± 0.5***

Figure 8. **Involvement of endogenous AGK in cell proliferation.** (A) PC-3 cells were transfected with control siRNA (open bars) or siAGK (hatched bars) and serum starved for 8 h. After culturing for an additional 16 h in serum-free medium or in medium supplemented with 10% serum, BrdU was added for 3 h and the fraction of cells incorporating BrdU was determined. Data are means ± SD of duplicate cultures from a representative experiment. At least three different fields were scored with a minimum of 100 cells per field. Similar results were obtained in two independent experiments. (B) Representative fluorescent and phase images of siControl and siAGK-transfected cells. (C) Cell cycle analysis. PC-3 cells transfected with control siRNA or siAGK were cultured in serum-free medium or in medium supplemented with 10% serum. After 24 h, cellular DNA was stained with propidium iodide and cell cycle analysis was performed with an Epics XL-MCL flow cytofluorometer (Beckman Coulter). Asterisks indicate significant differences from vector-transfected values as determined by *t* test ($P \leq 0.05$).

Discussion

Several lines of evidence suggest that AGK is a bona fide acylglycerol kinase. First, recombinant AGK catalyzes the phosphorylation of both MOG and DAG in vitro, producing LPA and PA, respectively. In agreement, bacterially expressed, purified recombinant AGK phosphorylated DAG as well as MOG (Waggoner et al., 2004). Second, overexpression of AGK increases cellular levels of LPA and PA. Third, and conversely, down-regulation of AGK reduces their intracellular levels. Fourth, overexpression of kinase dead AGK, although localized similarly to the mitochondria as wild-type AGK, does not increase acylglycerol kinase activity nor produce LPA.

Prostate carcinomas often possess an autocrine stimulatory loop in which the transformed cells express high levels of EGFR and also produce activating ligands. One such ligand might be the bioactive phospholipid LPA, which stimulates prostate cancer cell proliferation, migration, and survival, not only by acting on its cognate GPCRs but also by stimulating metalloproteinase activity and proteolytic EGF precursor processing leading to EGFR transactivation (Gschwind et al., 2001). Our identification of AGK as a lipid kinase that produces LPA and PA and is highly expressed in prostate tumors may have important clinical implications with regard to advanced prostate cancer. AGK not only regulates mitogenic EGFR signaling that plays important roles in androgen-refractory metastatic prostate cancer but also stimulates cell motility and EGFR-independent secretion of the pluripotent cytokine IL-8. Indeed, blockade of the EGFR in PC-3 cells inhibited tumor growth and invasion and also down-regulated expression of IL-8 within the tumors (Karashima et al., 2002).

Interestingly, the endocannabinoids anandamide and 2-AG potently inhibit proliferation and cause apoptosis of PC-3 and DU145 prostate cancer cells (Melck et al., 2000). Because AGK can phosphorylate 2-AG converting it to LPA, it may regulate the dynamic levels of these counterregulatory lipids that have been shown to play opposing roles in growth and survival of prostate cancers. Of note, LPA_3 was originally cloned from prostate cancer cells (Im et al., 2000), which is concordant with the ability of LPA to induce autocrine proliferation of these cells (Xie et al., 2002). Moreover, PC-3 cells express $LPA_{1\text{-}3}$ receptors, thus providing AGK with the potential to activate numerous downstream growth signaling pathways.

The mitogenic responses of some mammalian cells to LPA may be $LPA_{1\text{-}4}$ independent (Hooks et al., 2001). However, in prostate cancer cells, LPA transduces mitogenic signals via activation of $G_{\alpha i}$ and $G\beta\gamma$ subunits (Kue and Daaka, 2000; Bookout et al., 2003). Importantly, the expression of GRK2ct inhibited PC-3 tumor formation in animals (Bookout et al., 2003). Several lines of evidence indicate that the growth-promoting effects of AGK are mediated via LPA receptors. In RH7777 cells, which are devoid of $LPA_{1\text{-}4}$, expression of AGK had no effect on DNA synthesis, even in the presence of exogenous MOG. Moreover, PTX pretreatment decreased the growth-promoting effects of AGK. Our results are similar to others showing that PTX not only inhibits proliferation of PC-3 cells induced by LPA but also inhibits the effect of serum more drastically (Kue and Daaka, 2000). Furthermore, consistent with a previous study (Lea et al., 2004), GW9662, a selective antagonist of PPARγ, inhibited proliferation of vector-transfected PC-3 cells, and yet it did not abrogate the mitogenic effect of AGK. Our results are consistent with the notion that production and secretion of LPA by AGK induces Gi-dependent proliferation, likely through LPA receptors. Remarkably, down-regulation of AGK drastically reduced ERK1/2 activation induced by EGF, which, as expected, was bypassed by addition of the AGK product, LPA. Our data suggest that AGK plays an important role in EGF-induced mitogenic ERK signaling. AGK also phosphorylates DAG to produce the bioactive mediator PA, which regulates numerous biological processes including Raf translocation to the plasma membrane (Rizzo et al., 1999) and activation of mTOR (Fang et al., 2001). Our results also imply that specific pools of PA may play important roles in growth signaling.

Although the physiological function of LPA and PA generation in the mitochondria is not clear, a LPA phosphatase with 28.5% amino acid identity to human prostatic acid phosphatase is also localized to the mitochondria (Hiroyama and Takenawa, 1999). This LPA phosphatase has been suggested to regulate lipid metabolism in mitochondria by hydrolysis of LPA to monoacylglycerol (Hiroyama and Takenawa, 1999). Previous studies suggest that mitochondria-produced LPA can leave this organelle and be transported to the ER in the presence of liver fatty acid binding protein, can be secreted, and/or can be converted to PA (Haldar and Lipfert, 1990; Chakraborty et al., 1999; Hiroyama and Takenawa, 1999). In addition, LPA generated by prostate cancer cells in response to mitogenic stimuli can be secreted (Qi et al., 1998; Gibbs et al., 2000; Kue and Daaka, 2000; Kue et al., 2002; Xie et al., 2002).

It has been demonstrated that in both PC-3 and DU145 prostate cancer cells, agonists induce 18:1 LPA formation that is then released into the medium (Xie et al., 2002). As Du145 and PC-3 cells express $LPA_{1\text{-}3}$, it was suggested that 18:1 LPA can act as an autocrine mediator (Xie et al., 2002), yet the critical enzymes involved have not been identified. Our data suggest that AGK could be a missing link. Production of LPA by AGK, which in turn transactivates the EGFR, can amplify mitogenic and survival signals. Moreover, expression of AGK is stimulated by EGF, serum, and even by LPA itself, thereby providing a positive feed-forward stimulus that could further enhance EGFR-dependent and -independent processes important for cancer progression. Therefore, targeting AGK, which is upstream of the EGFR, could offer additional therapeutic benefits in treatment of androgen-independent prostate cancer.

Materials and methods

Cloning of an AGK

An EST (AW321722) was identified that contained an open reading frame with 25% identity and 50% similarity to hSphK2 from aa 133 to 256. 5′ and 3′ RACE were performed using the GeneRacer kit (Life Technologies) to obtain the sequence of the full-length open reading frame. A cDNA with a complete open reading frame was cloned from a human kidney cDNA library encoding a 422–amino acid polypeptide with a calculated molecular mass of 46,400 D (Fig. S1). A nearly identical mouse homologue (CAC06108) was also identified.

The predicted sequence of this human protein and its mouse homologue identified from the mouse database (CAC06108) are 95% identical and both show sequence similarity to SphKs, especially in the five conserved SphK domains (Liu et al., 2000, 2002). We previously noted that conserved regions 1–3 of SphKs have high sequence homology with the catalytic domain of DAGKs (DAGKc; Liu et al., 2002). This region (aa 65 to 191 of the new kinase) contains the $GDGXXXEXXXGXXXRX_nK$ ($n = 7$, 8) motif, present in the catalytic domain of SphKs (SphKc; Liu et al., 2002), which is reminiscent but distinct from the sequence GGDGXXG previously suggested to be part of the ATP binding site of DAGKc (Topham and Prescott, 1999). Of note, a lysine residue downstream of the glycine-rich region, which is conserved in the ATP binding sites of protein kinases (Hanks et al., 1988) and absent in DAGKc, is also present in SphKc and in this new lipid kinase (Fig. S1). However, Clustal W alignment revealed that hSphK1 and hSphK2 are more closely related to each other than to this new putative lipid kinase. Pairwise comparisons of the conserved subdomains of SphK1/SphK2, new lipid kinase/SphK1, new lipid kinase/SphK2, new lipid kinase/CERK, and new lipid kinase/DAGK indicated sequence identities of 53, 29, 23, 26, and 24%, respectively. These comparisons suggest that this new lipid kinase may be unique. A search of the human genome database revealed that the gene encoding this lipid kinase is located on chromosome 7q34, whereas SphK1 and SphK2 have been localized to chromosomes 17q25.2 and 19q13.2, respectively.

Cell culture and transfection

Human PC-3 prostate cancer cells (CRL-1435; American Type Culture Collection), NIH 3T3 fibroblasts (CRL-1658; American Type Culture Collection), rat hepatoma RH*7777* cells (provided by X. Fang, Virginia Commonwealth University, Richmond, VA), and human embryonic kidney cells (HEK 293; CRL-1573; American Type Culture Collection) were seeded at $4–5 \times 10^5$ cells per well in 6-well plates and transfected with Lipofectamine PLUS for NIH 3T3, HEK 293, and RH*7777* cells and Lipofectamine 2000 for PC-3 cells, according to the manufacturer's instructions (Life Technologies).

Catalytically inactive AGK

The QuikChange site-directed mutagenesis kit (Stratagene) was used to prepare catalytically inactive AGK (G126E) by mutating the conserved glycine in the glycine-rich loop of the ATP binding site (forward primer, 5′-TTGGAGGAGGAGATGAGACACTGCAGGAGGTT-3′, and reverse primer, 5′-AACCTCCTGCAGTGTCTCATCTCCTCCTGCAA-3′). The mutation was confirmed by sequencing.

siRNA transfection

AGK expression was down-regulated with sequence-specific siRNA. siRNA target sequence for AGK (siAGK: 5′-AACAGATGAGGCTACCTTCAG-3′) and control siRNA (5′-TTCTCCGAACGTGTCACGT-3′) were obtained from QIAGEN. In some experiments, cells were transfected with two additional AGK siRNAs ($siAGK_2$: 5′-GAGGCTACCTTCAGTAAGA-3′; $siAGK_3$: 5′-GGAGAGACCAGTAGTTTGA-3′) and siControl (non-targeting siRNA with at least four mismatches to all human and mouse genes from Dharmacon). Cells (3×10^5) were transfected in 6-well dishes for 3–4 h with the RNA duplexes (200 nM) using Oligofectamine (Life Technologies) according to the manufacturer's protocol. $90 \pm 2\%$ of the cells were transfected as determined with siGLO RISC-Free siRNA (Dharmacon).

Real-time PCR

Quantitative real-time PCR was performed on a real-time PCR machine (model Taqman ABI 7900; Applied Biosystems) with the following primers/probes: AGK forward primer, 5′-CGAAGGCTTGCGTCCTACTG-3′; reverse primer, 5′-TGGTGGACAGCTGCACATCT-3′; probe, 5′-CACAACCACAGGATGCCCTTTCCC-3′ (Integrated DNA Technologies); premixed primer-probe set for hSphK1 was purchased from Applied Biosystems. Ribosomal RNA (18S rRNA) measured using TaqMan assay reagents served as endogenous control.

Lipid kinase activity

Lipids (100 nmol) were dried under N_2 and resuspended in 180 μl of buffer containing 100 mM MOPS, pH 7.2, 2 mM EGTA, 15 mM NaF, 2 mM orthovanadate, 50 mM NaCl, 250 mM sucrose, 0.03% deoxycholate, and 1:500 diluted protease inhibitor cocktail (Sigma-Aldrich). After brief sonication, 10 μl lysates (10 μg) and 10 μl γ-[^{32}P]ATP (10 μCi, 1 mM) containing $MgCl_2$ (10 mM) were added and reactions were performed for 30 min at 37°C. ^{32}P-labeled lipids produced were extracted into 0.8 ml $CHCl_3$/MeOH/concentrated HCl (100:200:1, vol/vol), and phase separation was effected by adding 0.25 ml 2 M KCl and 0.25 ml $CHCl_3$. Aliquots of the organic phases were analyzed by TLC on silica gel G60 with $CHCl_3$/acetone/methanol/acetic acid/water (10:4:3:2:1, vol/vol) as solvent and the radioactive spots corresponding to migration of standards were quantified with an FX Molecular Imager (Bio-Rad Laboratories). In some experiments, SphK1 (Liu et al., 2000), SphK2 (Liu et al., 2000), ceramide, and DAGKs (Sugiura et al., 2002) were measured exactly as described.

AGK activity in immunoprecipitates

HEK 293 cells were seeded in 10-cm dishes and transiently transfected with vector or V5-tagged AGK. 24 h later, cells were lysed by sonication in buffer containing 100 mM MOPS, pH 7.2, 2 mM EGTA, 2 mM orthovanadate, 2 mM β-glycerophosphate, 150 mM NaCl, 250 mM sucrose, and 1:500 diluted protease inhibitor cocktail. Lysates were cleared by centrifugation and 400 μg of protein in 250 μl was incubated with 1 μg anti-V5 (Invitrogen) for 4 h at 4°C. Protein A/G PLUS–Agarose beads (10 μl; Santa Cruz Biotechnology, Inc.) were added and incubated for an additional 1 h. The beads were washed four times with the same buffer, resuspended in 10 μl, and AKG activity was determined.

^{32}P labeling of cellular phospholipids

Vector and kinase PC-3 transfectants were grown to 80–90% confluency in 100-mm dishes, incubated for 2 h with 40 μCi/ml ^{32}Pi in phosphate-free DME at 37°C, and washed and incubated for a further 2 h in 4 ml

phosphate-free DME. Medium was removed and after brief centrifugation lipids were extracted from a 3-ml aliquot of the medium by addition of 10.8 ml chloroform/methanol/concentrated HCl (100:200:1, vol/vol), followed by 3.6 ml each of chloroform and 2 M KCl. Lipids were also extracted from the cells after washing and scraping into 1.2 ml cold methanol/concentrated HCl (100:1), followed by addition of 0.6 ml chloroform. After vigorous vortexing, 0.6 ml $CHCl_3$ and 0.5 ml H_2O was added. Phases were separated by addition of 0.6 ml 2 M KCl. The organic phases were transferred to siliconized glass tubes and the aqueous phases reextracted with 0.6 ml $CHCl_3$. Aliquots containing 50,000 cpm were separated by two-dimensional TLC (Yokoyama et al., 2000). Radioactive spots were identified by comparison to standard phospholipids and quantified with a phosphoimager. In some experiments, phospholipids were separated by one-dimensional TLC using $CHCl_3$/methanol/water/ammonium hydroxide (120:75:6:2, vol/vol; Liu et al., 2003).

Northern analysis and matched tumor/normal expression array
Poly(A)$^+$ RNA blot of multiple adult human tissues (CLONTECH Laboratories, Inc.) was used for Northern blotting analysis of AGK expression. The blot was hybridized with a probe prepared by labeling the PCR product with γ-[^{32}P]dCTP in ExpressHyb buffer (CLONTECH Laboratories, Inc.) at 65°C overnight. A matched tumor/normal expression array (CLONTECH Laboratories, Inc.) was similarly probed with radiolabeled full-length AGK.

Chemotactic motility
Chemotaxis was measured in a modified Boyden chamber using collagen-coated polycarbonate filters (25 × 80 mm, 8-μM pore size) as previously described (Wang et al., 1999).

In vitro wound closure assay
Confluent monolayers of PC-3 cells were serum starved for 24 h, wounded by making a uniform scratch with a pipet tip, and washed to remove detached cells. Wound closure was monitored after 24 h in serum-free medium by determining the number of cells migrating into the wound using ImagePro Plus software to analyze digital images from an inverted phase microscope.

Cell proliferation assays
PC-3 cell proliferation was determined with crystal violet (Olivera et al., 1999). In some experiments, cell growth was measured by adding WST-1 reagent (Roche) and incubating at 37°C for 3 h. Absorbance was measured at 450 nm with background subtraction at 650 nm. BrdU incorporation and analysis of cell cycle profile by flow cytometry were performed exactly as described previously (Olivera et al., 1999).

IL-8 secretion
PC-3 cells were serum starved overnight, and after stimulation in serum-free DME for 16 h, media was collected and briefly centrifuged to remove cells. Secreted IL-8 was determined with the Quantikine IL-8 ELISA kit (R&D Systems).

Immunofluorescence and confocal microscopy
Cells were grown on glass coverslips and transfected with vector or V5-tagged AGK. 24 h later, cells were incubated with 200 nM MitoTracker red CMXRos (Molecular Probes) to stain mitochondria and fixed in 3% PFA in PBS containing 0.1% Triton X-100. ER was visualized with polyclonal rabbit anti-calnexin antibody followed by anti–rabbit IgG-FITC. Transfected cells were visualized simultaneously with anti-V5 antibody (1:500; Invitrogen) followed by a secondary anti–mouse antibody conjugated with FITC or Texas red (Molecular Probes), respectively. Coverslips were mounted on glass slides using an Anti-Fade kit (Molecular Probes) and examined by confocal microscopy. Images were collected with a laser scanning microscope (model IX70; Olympus) equipped with argon (488 nm) and krypton (568 and 647 nm) lasers and a 60×/1.4 NA PlanApo lens. Quantitative image analysis was performed using Metamorph image processing software.

Subcellular fractionation
Cells transfected with vector or AGK were Dounce homogenized in buffer containing 20 mM Hepes, pH 7.4, 10 mM KCl, 2 mM $MgCl_2$, 1 mM EDTA, 250 mM sucrose, 10 μg/ml aprotinin, 10 μg/ml leupeptin, and 1 mM PMSF. Subcellular fractionation was performed by differential centrifugation at 4°C as described previously (Le Stunff et al., 2002). In brief, lysates were centrifuged at 1000 *g* for 5 min to remove unbroken cells and nuclei (P1, nuclei and unbroken cells); postnuclear supernatants were centrifuged at 5,000 *g* for 10 min (P2, mitochondria); followed by 17,000 *g* for 15 min (P3, intracellular membrane fraction containing ER and Golgi). The remaining supernatant was centrifuged at 100,000 *g* for 1 h to obtain plasma membranes. Proteins were separated by SDS-PAGE, transferred to nitrocellulose membranes, and probed with antibodies as described in the figure legends.

Immunoprecipitation
PC-3 cells were lysed in buffer containing 25 mM Hepes, pH 7.5, 0.3 M NaCl, 1.5 mM $MgCl_2$, 0.2 mM EDTA, 1% Triton X-100, 0.5% sodium deoxycholate, 0.1% SDS, 20 mM β-glycerophosphate, 1 mM sodium orthovanadate, 0.5 mM dithiothreitol, 1 mM PMSF, and 10 μg/ml leupeptin. Lysates were cleared by centrifugation at 10,000 *g* for 10 min and incubated with 2 μg anti-EGFR antibody for 2 h at 4°C. 20 μl of protein A/G–Sepharose beads (Santa Cruz Biotechnology, Inc.) were added and incubated for an additional 1 h at 4°C. Sepharose beads were washed and boiled in SDS sample buffer, and bound proteins were analyzed by Western blotting.

Online supplemental material
Fig. S1 shows a Clustal W alignment of AGK with other lipid kinases. Fig. S2 demonstrates the mitochondrial localization of AGK and catalytically inactive AGK and confirms that the mutant has no kinase activity. Fig. S3 shows the effect of AGK on growth and survival of NIH 3T3 cells. Fig. S4 shows regulation of EGFR phosphorylation by AGK. Online supplemental material is available at http://www.jcb.org/cgi/content/full/jcb.200407123/DC1.

We thank Dr. Xianjun Fang for helpful discussions.

This work was supported by grants from the National Institutes of Health (R01CA61774) and the Department of Defense (DAMD17-02-1-0060) to S. Spiegel.

Submitted: 19 July 2004
Accepted: 14 April 2005

References

Baker, D.L., D.M. Desiderio, D.D. Miller, B. Tolley, and G.J. Tigyi. 2001. Direct quantitative analysis of lysophosphatidic acid molecular species by stable isotope dilution electrospray ionization liquid chromatography-mass spectrometry. *Anal. Biochem.* 292:287–295.

Bookout, A.L., A.E. Finney, R. Guo, K. Peppel, W.J. Koch, and Y. Daaka. 2003. Targeting Gbetagamma signaling to inhibit prostate tumor formation and growth. *J. Biol. Chem.* 278:37569–37573.

Bunting, M., W. Tang, G.A. Zimmerman, T.M. McIntyre, and S.M. Prescott. 1996. Molecular cloning and characterization of a novel human diacylglycerol kinase ζ. *J. Biol. Chem.* 271:10230–10236.

Chakraborty, T.R., A. Vancura, V.S. Balija, and D. Haldar. 1999. Phosphatidic acid synthesis in mitochondria. Topography of formation and transmembrane migration. *J. Biol. Chem.* 274:29786–29790.

Fang, Y., M. Vilella-Bach, R. Bachmann, A. Flanigan, and J. Chen. 2001. Phosphatidic acid-mediated mitogenic activation of mTOR signaling. *Science.* 294:1942–1945.

Fukushima, N., Y. Kimura, and J. Chun. 1998. A single receptor encoded by vzg-1/lpA1/edg-2 couples to G proteins and mediates multiple cellular responses to lysophosphatidic acid. *Proc. Natl. Acad. Sci. USA.* 95:6151–6156.

Gibbs, T.C., Y. Xie, and K.E. Meier. 2000. Regulation of expression of EDG family receptors in human prostate cancer cell lines. *Ann. NY Acad. Sci.* 905:290–293.

Gschwind, A., E. Zwick, N. Prenzel, M. Leserer, and A. Ullrich. 2001. Cell communication networks: epidermal growth factor receptor transactivation as the paradigm for interreceptor signal transmission. *Oncogene.* 20:1594–1600.

Haldar, D., and L. Lipfert. 1990. Export of mitochondrially synthesized lysophosphatidic acid. *J. Biol. Chem.* 265:11014–11016.

Hanks, S.K., A.M. Quinn, and T. Hunter. 1988. The protein kinase family: conserved features and deduced phylogeny of the catalytic domains. *Science.* 241:42–51.

Hiroyama, M., and T. Takenawa. 1999. Isolation of a cDNA encoding human lysophosphatidic acid phosphatase that is involved in the regulation of mitochondrial lipid biosynthesis. *J. Biol. Chem.* 274:29172–29180.

Hooks, S.B., W.L. Santos, D.S. Im, C.E. Heise, T.L. Macdonald, and K.R. Lynch. 2001. Lysophosphatidic acid-induced mitogenesis is regulated by lipid phosphate phosphatases and is Edg-receptor independent. *J. Biol. Chem.* 276:4611–4621.

Im, D.S., C.E. Heise, M.A. Harding, S.R. George, B.F. O'Dowd, D. Theodorescu,

and K.R. Lynch. 2000. Molecular cloning and characterization of a lysophosphatidic acid receptor, Edg-7, expressed in prostate. *Mol. Pharmacol.* 57:753–759.

Karashima, T., P. Sweeney, J.W. Slaton, S.J. Kim, D. Kedar, J.I. Izawa, Z. Fan, C. Pettaway, D.J. Hicklin, T. Shuin, and C.P. Dinney. 2002. Inhibition of angiogenesis by the antiepidermal growth factor receptor antibody ImClone C225 in androgen-independent prostate cancer growing orthotopically in nude mice. *Clin. Cancer Res.* 8:1253–1264.

Kim, S.J., H. Uehara, T. Karashima, M. McCarty, N. Shih, and I.J. Fidler. 2001. Expression of interleukin-8 correlates with angiogenesis, tumorigenicity, and metastasis of human prostate cancer cells implanted orthotopically in nude mice. *Neoplasia.* 3:33–42.

Kue, P.F., and Y. Daaka. 2000. Essential role for G proteins in prostate cancer cell growth and signaling. *J. Urol.* 164:2162–2167.

Kue, P.F., J.S. Taub, L.B. Harrington, R.D. Polakiewicz, A. Ullrich, and Y. Daaka. 2002. Lysophosphatidic acid-regulated mitogenic ERK signaling in androgen-insensitive prostate cancer PC-3 cells. *Int. J. Cancer.* 102:572–579.

Le Stunff, H., I. Galve-Roperh, C. Peterson, S. Milstien, and S. Spiegel. 2002. Sphingosine-1-phosphate phosphohydrolase in regulation of sphingolipid metabolism and apoptosis. *J. Cell Biol.* 158:1039–1049.

Lea, M.A., M. Sura, and C. Desbordes. 2004. Inhibition of cell proliferation by potential peroxisome proliferator-activated receptor (PPAR) gamma agonists and antagonists. *Anticancer Res.* 24:2765–2771.

Liu, H., M. Sugiura, V.E. Nava, L.C. Edsall, K. Kono, S. Poulton, S. Milstien, T. Kohama, and S. Spiegel. 2000. Molecular cloning and functional characterization of a novel mammalian sphingosine kinase type 2 isoform. *J. Biol. Chem.* 275:19513–19520.

Liu, H., D. Chakravarty, M. Maceyka, S. Milstien, and S. Spiegel. 2002. Sphingosine kinases: a novel family of lipid kinases. *Prog. Nucleic Acid Res. Mol. Biol.* 71:493–511.

Liu, J., Q. Dai, J. Chen, D. Durrant, A. Freeman, T. Liu, D. Grossman, and R.M. Lee. 2003. Phospholipid scramblase 3 controls mitochondrial structure, function, and apoptotic response. *Mol. Cancer Res.* 1:892–902.

Melck, D., L. De Petrocellis, P. Orlando, T. Bisogno, C. Laezza, M. Bifulco, and V. Di Marzo. 2000. Suppression of nerve growth factor Trk receptors and prolactin receptors by endocannabinoids leads to inhibition of human breast and prostate cancer cell proliferation. *Endocrinology.* 141:118–126.

Mills, G.B., and W.H. Moolenaar. 2003. The emerging role of lysophosphatidic acid in cancer. *Nat. Rev. Cancer.* 3:582–591.

Olivera, A., T. Kohama, L.C. Edsall, V. Nava, O. Cuvillier, S. Poulton, and S. Spiegel. 1999. Sphingosine kinase expression increases intracellular sphingosine-1-phosphate and promotes cell growth and survival. *J. Cell Biol.* 147:545–558.

Pieringer, R.A., and L.E. Hokin. 1962. Biosynthesis of lysophosphatidic acid from monoacylglyceride and adenosine triphosphate. *J. Biol. Chem.* 237:653–658.

Pitson, S.M., P.A. Moretti, J.R. Zebol, R. Zareie, C.K. Derian, A.L. Darrow, J. Qi, R.J. D'Andrea, C.J. Bagley, M.A. Vadas, and B.W. Wattenberg. 2002. The nucleotide-binding site of human sphingosine kinase 1. *J. Biol. Chem.* 277:49545–49553.

Prenzel, N., E. Zwick, H. Daub, M. Leserer, R. Abraham, C. Wallasch, and A. Ullrich. 1999. EGF receptor transactivation by G-protein-coupled receptors requires metalloproteinase cleavage of proHB-EGF. *Nature.* 402:884–888.

Qi, C., J.H. Park, T.C. Gibbs, D.W. Shirley, C.D. Bradshaw, K.M. Ella, and K.E. Meier. 1998. Lysophosphatidic acid stimulates phospholipase D activity and cell proliferation in PC-3 human prostate cancer cells. *J. Cell. Physiol.* 174:261–272.

Raj, G.V., L. Barki-Harrington, P.F. Kue, and Y. Daaka. 2002. Guanosine phosphate binding protein coupled receptors in prostate cancer: a review. *J. Urol.* 167:1458–1463.

Rizzo, M.A., K. Shome, C. Vasudevan, D.B. Stolz, T.C. Sung, M.A. Frohman, S.C. Watkins, and G. Romero. 1999. Phospholipase D and its product, phosphatidic acid, mediate agonist-dependent raf-1 translocation to the plasma membrane and the activation of the mitogen-activated protein kinase pathway. *J. Biol. Chem.* 274:1131–1139.

Shim, Y.H., C.H. Lin, and K.P. Strickland. 1989. The purification and properties of monoacylglycerol kinase from bovine brain. *Biochem. Cell Biol.* 67:233–241.

Simpson, C.M., H. Itabe, C.N. Reynolds, W.C. King, and J.A. Glomset. 1991. Swiss 3T3 cells preferentially incorporate sn-2-arachidonoyl monoacylglycerol into sn-1-stearoyl-2-arachidonoyl phosphatidylinositol. *J. Biol. Chem.* 266:15902–15909.

Sugiura, M., K. Kono, H. Liu, T. Shimizugawa, H. Minekura, S. Spiegel, and T. Kohama. 2002. Ceramide kinase, a novel lipid kinase. Molecular cloning and functional characterization. *J. Biol. Chem.* 277:23294–23300.

Sugiura, T., S. Kondo, S. Kishimoto, T. Miyashita, S. Nakane, T. Kodaka, Y. Suhara, H. Takayama, and K. Waku. 2000. Evidence that 2-arachidonoylglycerol but not N-palmitoylethanolamine or anandamide is the physiological ligand for the cannabinoid CB2 receptor. Comparison of the agonistic activities of various cannabinoid receptor ligands in HL-60 cells. *J. Biol. Chem.* 275:605–612.

Topham, M.K., and S.M. Prescott. 1999. Mammalian diacylglycerol kinases, a family of lipid kinases with signaling functions. *J. Biol. Chem.* 274: 11447–11450.

Umezu-Goto, M., Y. Kishi, A. Taira, K. Hama, N. Dohmae, K. Takio, T. Yamori, G.B. Mills, K. Inoue, J. Aoki, and H. Arai. 2002. Autotaxin has lysophospholipase D activity leading to tumor cell growth and motility by lysophosphatidic acid production. *J. Cell Biol.* 158:227–233.

Waggoner, D.W., L.B. Johnson, P.C. Mann, V. Morris, J. Guastella, and S.M. Bajjalieh. 2004. MuLK: A novel eukaryotic multi-substrate lipid kinase. *J. Biol. Chem.* 279:38228–38235.

Wang, F., J.R. Van Brocklyn, L. Edsall, V.E. Nava, and S. Spiegel. 1999. Sphingosine-1-phosphate inhibits motility of human breast cancer cells independently of cell surface receptors. *Cancer Res.* 59:6185–6191.

Xie, Y., T.C. Gibbs, Y.V. Mukhin, and K.E. Meier. 2002. Role for 18:1 lysophosphatidic acid as an autocrine mediator in prostate cancer cells. *J. Biol. Chem.* 277:32516–32526.

Yokoyama, K., F. Shimizu, and M. Setaka. 2000. Simultaneous separation of lysophospholipids from the total lipid fraction of crude biological samples using two-dimensional thin-layer chromatography. *J. Lipid Res.* 41:142–147.

Zhang, C., D.L. Baker, S. Yasuda, N. Makarova, L. Balazs, L.R. Johnson, G.K. Marathe, T.M. McIntyre, Y. Xu, G.D. Prestwich, et al. 2004. Lysophosphatidic acid induces neointima formation through PPARγ activation. *J. Exp. Med.* 199:763–774.